UNCLASSIFIED

AEC
RESEARCH AND
DEVELOPMENT REPORT

NYO 9061

UC-25 METALLURGY AND CERAMICS
TID-4500 14th Ed.

FUEL ELEMENT DEVELOPMENT PROGRAM

FOR THE

PEBBLE BED REACTOR

QUARTERLY PROGRESS REPORT

May 1, 1960 to July 31, 1960

SANDERSON & PORTER

NEW YORK, N.Y.

Price $1.50. Available from the Office of Technical Services, Department of Commerce, Washington 25, D.C.

DISCLAIMER

NYO 9061
AEC Research and
Development Report
UC-25, Metallurgy &
Ceramics
TID 4500, 14th. Ed.

FUEL ELEMENT DEVELOPMENT PROGRAM

for the

PEBBLE BED REACTOR

QUARTERLY PROGRESS REPORT

May 1 to July 31, 1960

Work Performed Under AEC Contract AT(30-1)-2378

SANDERSON & PORTER

NEW YORK, N. Y.

TABLE OF CONTENTS

Summary and Conclusions

A Pebble Bed Reactor fuel element specimen (i.e. a 1 1/2 inch graphite sphere fueled with vapor deposited alumina coated UO_2) achieved a burnup of 3.3 a/o U235 during 84 days of irradiation in Sweep Capsule SP-5 at 1.5 KW and 1400°F average temperature. Up to about 2.5 a/o burnup the fission product leakage factors (i.e. rate of release/rate of production) for ten isotopes varying in half life from 5.27d Xe133 to 1.7s Xe141 ranged between 10^{-9} and 10^{-5}. These leakage factors were somewhat temperature dependent. Since the leakage factors were approximately equal for isotopes having such a variation in half life, it is concluded that the "leakage" was due to trace amounts of uranium contamination outside the particle coatings. During the latter part of the quarter, the leakage factor for the longer lived Xe133 rose to 10^{-3} while several shorter lived fission products increased to a lesser extent. It is concluded that this indicates measurable diffusion starting to occur through the fuel particle coatings due to a radiation damage effect to the alumina. This pattern of fission product leakage could still prove to be acceptable to a large scale reactor since practically all of the non-volatile fission products which cause maintenance problems in primary loop equipment are daughters of the shorter-lived gaseous fission products.

The excellent results obtained from this specimen has fulfilled the early promise shown by this new type of coating material which can be called a "molecularly deposited ceramic". In addition to vapor deposited alumina, pyrolytically deposited carbon coatings on fuel particles have also been studied. It is probable that these two materials are forerunners of a variety of ceramic materials which will make it possible to produce high temperatures while at the same time achieving the low activity levels of metal clad fuel element systems.

Further development work with alumina coatings has shown no apparent problems in coating thoria bearing particles. The first attempts were successful in fabricating a coated particle containing a porous inner layer of alumina which could provide additional residence space for fission product gases. Some reaction has been found between alumina and graphite at 2500°F which indicates that tests will have to be performed at lower temperatures to establish the safe maximum temperature. The fission product retention ability of alumina above 1500°F remains to be explored in Furnace Capsule SPF-3. An impact test on a sphere fueled with thick

alumina coating (coating thickness approximately equal to the particle diameter) which were made by a previously studied sintering process (3) showed no damage to the particle coatings after sphere fracture.

Pyrolytic carbon coated fuel particles are of interest because there will be no temperature limitation imposed by reaction with the graphite matrix, and there is no displacement of moderator by the presence of the coating. UC_2 particles coated with pyrolytic carbon at 2000°F have been shown to have good fission product retention by the Neutron Activation screening test up to 2000°F. Less than 4.5×10^{-6} of the Xe133 was released in a 4 hr test. Beyond the deposition temperature, the coatings are found to crack because of the higher expansion coefficient of the UC_2. One solution to this problem is the use of higher deposition temperatures. Thermal cycle tests of particles coated at 2450°F showed significantly less failures when heated to 3600°F compared with the particles coated at 2000°F. A more rapid deposition rate and an absence of excess soot formation was also noted in fabricating the 2450°F material. Some damage to the 2000°F pyrolytic carbon coated fuel particles was noted when these particles were mixed and molded into graphite spheres. Although these particles were irregular in shape, further work on the effect of each fabrication step on particle coating integrity is warranted.

Graphite bodies in excess of 2.0 gm/cc density have been prepared without resorting to carbonaceous reimpregnation by using natural graphite powder as the filler material. Best results were obtained with a Madagascar crystalline graphite and small amounts of phenolic resin binder. Crushing strengths of these natural graphite pellets were of the same order as crushing strengths of AGOT (synthetic) graphite. The suitability of natural graphite in the form of graphite spheres remains to be explored next quarter.

Subassembly fabrication of an in-pile loop to study the behaviour of fission products in a recycled helium stream was completed this quarter. Irradiation of a graphite sphere fueled with alumina coated UO_2 will begin next quarter.

Results to date in the Pebble Bed Reactor Fuel Element Development Program have shown that the concept of a simple, rugged graphite sphere as a economical high temperature fuel element has been given major impetus by the use of molecularly deposited ceramic coatings on the fuel particles to retain fission products. This concept will continue to receive major emphasis during the remainder of the present Program.

1.0 Introduction

The basic objective of the Pebble Bed Reactor Fuel Element Development Program is to develop and/or evaluate fuel elements which would be suitable for the economic operation of a large scale Pebble Bed Reactor. The characteristics of a reference design fuel element have been based on design studies of a 125 eMW Pebble Bed Reactor Steam Power Plant (1, 2). This reactor is a high temperature, all-ceramic, helium-cooled reactor, consisting of a randomly packed static bed of fueled graphite spheres. Fuel element characteristics have been completely described in the Phase I Report on the PBR Fuel Element Development Program (3) and are summarized below.

1. The fuel element is a 1-1/2 inch diameter sphere of fueled graphite.
2. Fuel loading is 4.75 gms of uranium in the form of either the oxide or the carbide.
3. The maximum power density is 3 KW per sphere. Maximum surface and center temperature are 1800°F and 2100°F respectively. The design burnup is 5500 KWH per sphere which is equivalent to 6 a/o of total uranium or 40,000 MWD/metric ton of uranium.
4. Fission product retention should be such that the external activity level is less than 10^{-6} of the activity which would result from the complete release of all isotope chains containing volatile fission products.
5. The spheres shall withstand a 2.0 ft-lb impact load and a 500 lb. compressive load.
6. Other pertinent features are that adjacent fuel elements should not self-weld, fuel element coatings should withstand internal pressure buildup of gaseous fission products, and fuel element surfaces should not dust, abrade of erode.

The PBR Fuel Element Development Program has been arranged to evaluate these various characteristics. In general, fuel element specimens are subjected to pre-irradiation testing, followed by irradiation tests to measure fission product retention characteristics and/or the effects of irradiation on physical properties. Final steps in the program include the operation of an in-pile loop to simulate problems in the primary loop of a Pebble Bed Reactor. The test apparatus used in this program has been

described in reference (3). All phases of the evaluation program up to and including the capsule irradiations are being conducted at the Battelle Memorial Institute. The in-pile loop program is being conducted by the Nuclear Science and Engineering Corporation.

The present report describes the results of the PBR Fuel Element Development Program during the period from May through July, 1960 which was the fifth quarterly period of a two year program. Previous pertinent reports are the Phase I Report (3) covering the first two quarters, the third quarterly report (4), and the fourth quarterly report (5).

A significant shift in emphasis within the PBR Fuel Element Development Program had occurred during the previous quarter. Whereas a wide variety of surface coatings for the graphite spheres which might retain fission products were being evaluated, several developments caused the emphasis to shift to coatings on individual fuel particles as the primary barrier to fission product leakage (5). The advantages of coatings on fuel particles include retention of fission products at their source; the large thickness-to-diameter ratio of the ceramic material makes it less subject to physical damage; and the fracture of a PBR fuel element will not expose uncoated fuel particles.

One important characteristic of the particle coatings in the PBR Fuel Element Program is their method of fabrication. These particle coatings represent a new type of ceramic material which could be called a "molecularly deposited ceramic". In general, these new ceramics appear to have much lower permeability and much higher strength than conventional ceramics. Most of the work to date has been with vapor deposited alumina (Al_2O_3) on UO_2 particles. Another material under development is pyrolytic carbon on UC_2 particles. Both of these coating materials are deposited on the fuel particle surfaces from a gas phase reaction.

Most of the work during this quarter involved these two types of coated particles. Several PBR fuel element specimens have been made with these coated particles. A description of these specimens together with earlier specimens still under evaluation is given in Table 1-1. The manufacturer and pertinent characteristics of the fuel elements are listed. Each type of specimen has been assigned a type number.

TABLE 1-1

Summary of PBR Fuel Element Types

Number	FA-1	FA-20	FA-22	FA-23	FA-24
Mfgr.	Nat Carb.	Nat Carb.	Nat Carb.(1)	3M	Carbo.(1)
FUEL					
Loaded As	UO_2	UO_2	UO_2	UO_2	UC_2
Final Form	UO_2	UC_2	UO_2	UC	UC_2
Particle Size, μ	100/150	100/150	100/150	100/200	100/150
MATRIX					
Reimpreg.	no	no	no	yes	no
Net Density	1.62	1.65	1.57	1.75	1.55
Shell Thick.	0	0	0	.125"	0
Bake Temp, °F	2560	4800	2300	3600	2000
COATING					
Location	——	Surf.	Part.	Surf.	Part.
Material	——	Pyro-C	Al_2O_3	SiC-Si	Pyro-C
Thickness	——	.002"	50μ	.003"	40 μ

(1) Fuel particles coated by Battelle Memorial Institute.

Numbers are assigned serially and have no special significance. Occasionally, when it is desired to identify a particular ball within a group, an additional identification number in parentheses will be added to the type number.

Work on alumina coated particles is described in two sections: fabrication and screening tests in Section 2.0 and high level irradiation tests in Section 4.0. Work on pyrolytic carbon coated particles is described in Section 3.0. Two other facets of the PBR Fuel Element Program are also described. These are the development of high density graphite bodies made from natural graphite rather than the more common synthetic graphite (Section 5.0) and an in-pile loop where the behaviour of fission products in a recycled helium stream will be studied (section 6.0).

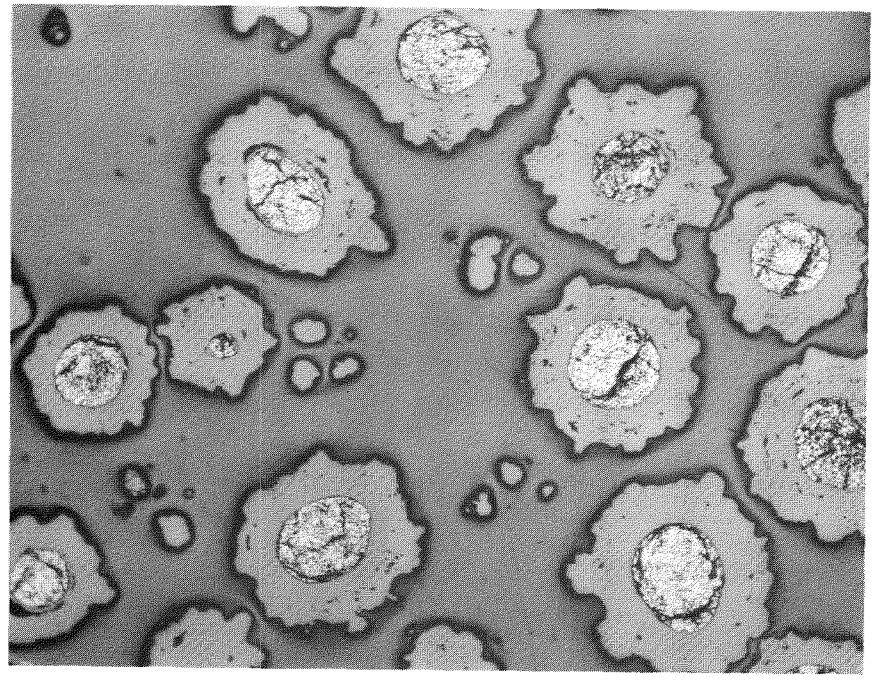

Fig. 2-1. Batch 6F showing Al_2O_3 Coatings on UO_2 (100X).

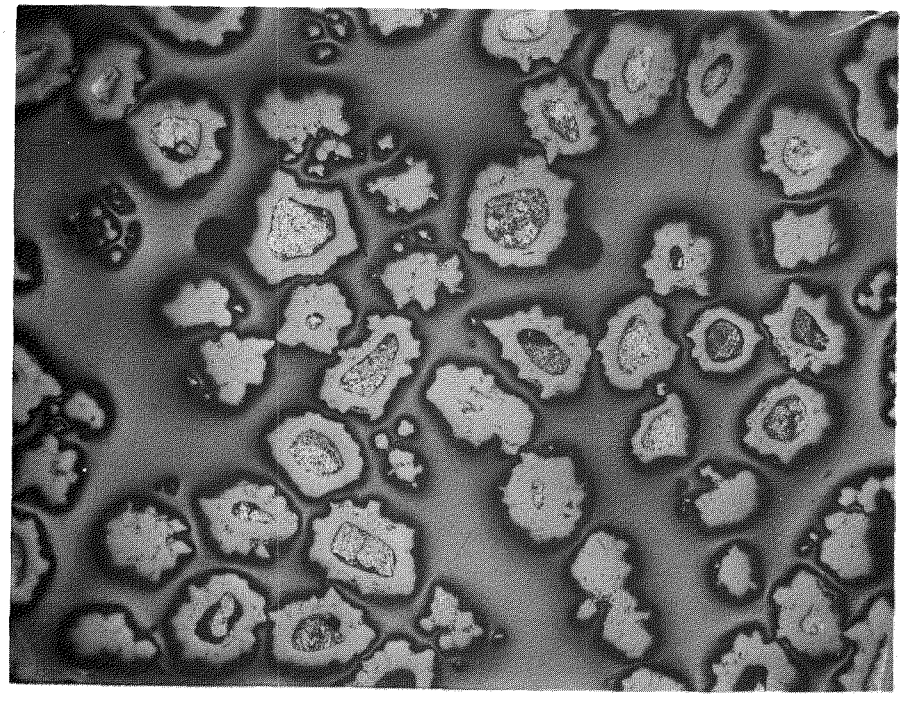

Fig. 2-2. Batch 7H showing Al_2O_3 coatings on ThO_2/UO_2 particles (50X).

ThO_2/UO_2 particles are somewhat irregular, all particles are seen to be adequately coated with no evidence of gaps between successive coating layers.

Batch 8G was prepared with two special features in mind: (1) a large UO_2 particles was used (297/350 micron) so that a thick coating could be applied and not exceed limitations on carbon moderator displacement when dispersed in a graphite sphere, and (2) a porous inner layer of alumina was used which would have the advantage of providing a reservior for fission gases and a cushion to prevent thermal cycle fracture of the outermost impermeable alumina coating. A thin 2 micron coating was first deposited at 1830°F so that any uranium contamination arising from dusting of the bare UO_2 particles during the early stages of fluidization could be leached away. Next, a 20 micron layer of porous Al_2O_3 was deposited at 1380°F. Additional impermeable alumina was deposited at 1830°F until a total alumina thickness of 150 microns was reached. 5 gm. samples were removed from the batch at coating thickness of 30, 50, 77, 106, 122 and 150 microns in order to evaluate the effect of coating thickness of thermal cycle rupture. Fig. 2-3 shows a particle from batch 8A which has been coated with only the thin impermeable layer and the porous layer of alumina. Fig. 2-4 shows several particles from the final batch, 8G. The dark band near the UO_2 particle is the porous alumina. Some evidence of annular porosity in the UO_2 particles can be noted. Occasional growths of alumina can be seen to protrude from the outer surface of the coating. In several instances, a dust particle inclusion can be noted at the base of the alumina growths. Similar growths have been noted in pyrolytically deposited carbon coatings which were also believed to arise from soot particles.

This completion of batch 8G concludes the exploratory work on alumina fabrication under the Pebble Bed Reactor Program. During the next quarter, several batches of alumina coated enriched UO_2 particles will be prepared for irradiation testing.

2.2 Pre-Irradiation Testing of Alumina Coated Particles

A number of standard screening tests are used for alumina coated fuel particles. In general, each batch of particles which has been fabricated is subjected to the following tests:

1. Alpha Assay: Uranium contamination on the surface of the particles is detected by placing a thin layer of the coated particles in a 2π proportional

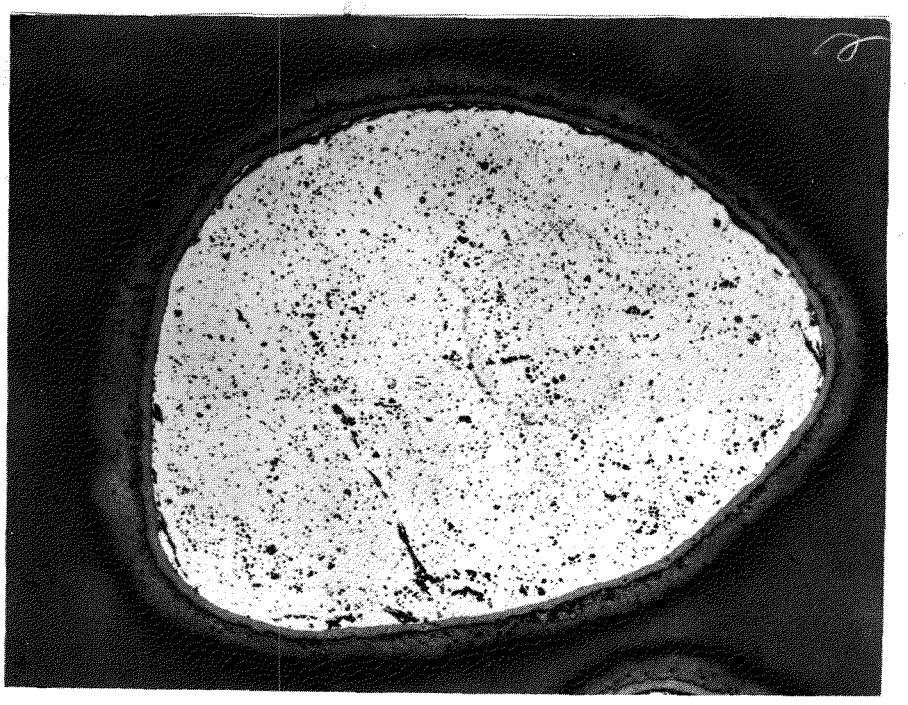

Fig. 2-3. Batch 8A showing thin impermeable layer of Al_2O_3 and porous layer of Al_2O_3 on UO_2 particle (500X).

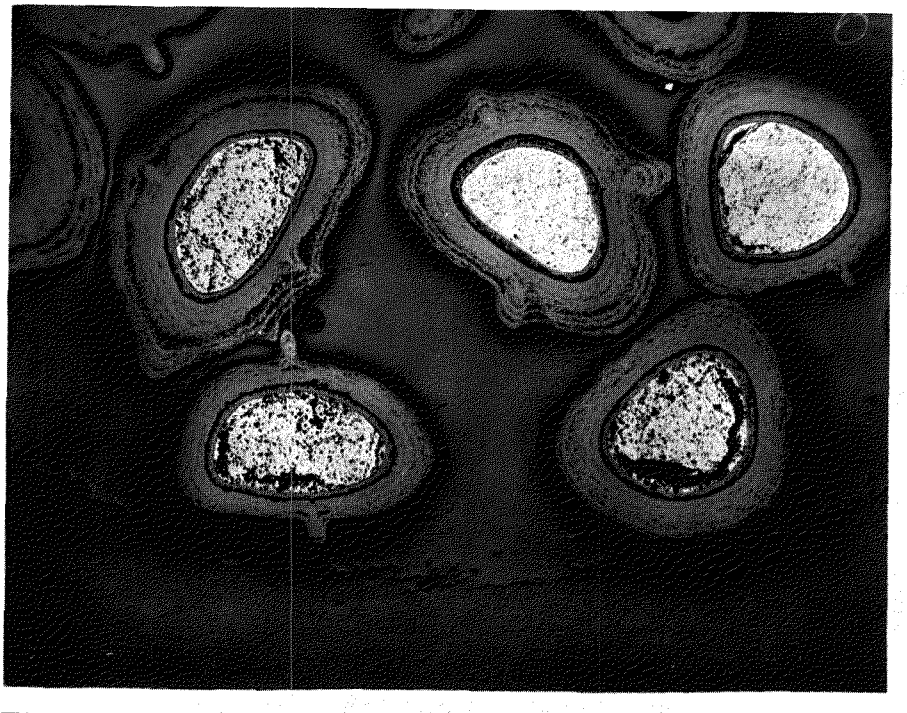

Fig. 2-4. Batch 8G showing Al_2O_3 coating with porous inner layer on UO_2 (50X).

gas flow counter and measuring the alpha emission rate.

2. Coating Integrity: Coated particles are exposed to air at 1200°F. Any faults in the coating cause the underlying UO_2 to be oxidized to U_3O_8 which further ruptures the coating due to expansion of the fuel particle. Thus, weight gain after this test is a measure of lack of coating integrity. An entire batch of particles can be subjected to this test so that faulty particles can be subsequently removed by leaching.

3. Thermal Cycling: Particles are thermal cycled between room temperature and 2500°F in an inert atmosphere to determine whether the slightly higher expansion coefficient of UO_2 as compared with the alumina coating will cause the coating to fail when the particle is heated above its fabrication temperature.

4. Metallographic Examination: Routine metallography is done up to 500X. On occasion, electron microscopy is used for more detailed study.

An additional screening test which was started during the previous quarter is the carburization test in which alumina coated particles mounted in a graphite matrix are heated at 2500°F for varying lengths of time to determine the extent of reaction between alumina and various types of graphite.

Batches 6F and 6H. A summary of the pre-irradiation evaluation results for the enriched UO_2 particles coated with alumina are given in Table 2-2.

TABLE 2-2

Evaluation of Batches 6F and 6H, Fueled with Enriched UO_2

Batch No.	6F	6H
Coating Thickness, μ	42	48
UO_2 Content, w/o	27.3	26.6
Coating Integrity Test:		
Batch Size, gms	109	125
Weight Change in 5 hrs, gms	+0.0004	-0.0410
Alpha Assay, As-Fab:		
Net α cpm/gm. sample	0.4 ± 1.2	0.4 ± 1.2
Equiv. U, mg/gm sample	.00011	.00011

As can be noted in Table 2-2, the quality of these coatings is excellent. The weight changes after the air oxidation test are insignificant. It should be recalled that similar tests on other types of particle coatings would often show 1% to 10% weight gains. The slight weight loss seen for batch 6H is unexplained but most probably due to devolatilization of air or moisture adsorbed prior to the heating test. No physical significance can be attached to the results of the alpha assay except that the uranium contamination is so low that it is at or below the limit of measurement by this method. It should be noted that if there were to be complete fission product release from only the 0.00011 mg. U per gm of sample, the fission product leakage factor (R/B) would be 10^{-7}.

Batches 7H and 7J. A summary of the pre-irradiation evaluation results for the ThO_2/UO_2 particles coated with alumina is given in Table 2-3.

TABLE 2-3

Evaluation of Batches 7H and 7J, Fueled with ThO_2/UO_2

Batch No.	7H	7J
Coating Thickness, μ	40	44
UO_2 Content, w/o	2.43	2.39
ThO_2 Content, w/o	33.0	32.1
Coating Integrity Test:		
Batch Size, gms	89	132
Weight Change in 5 hrs, gms	-0.0005	nil
Alpha Assay, As-Fab:		
Net α cpm/gm sample	2.0 ± 0.4	0.5 ± 1.0
Equiv. U, mg/gm sample	$.00\overline{27}$	$.00\overline{067}$
Alpha Assay, After Thermal Cycle:		
Net α cpm/gm sample	5.9 ± 2.0	0.4 ± 0.8
Equiv. U + Th, mg/gm sample	$.00\overline{79}$	$.00\overline{054}$

Again, the quality of the coatings on batches 7H and 7J according to both the air oxidation test and the alpha assay is seen to be excellent. The thermal cycle test has shown no significant effect on these coatings. From these examinations, it can be concluded that thoria bearing particles can be satisfactorily coated with alumina.

Batches 8A-8G. A summary of the pre-irradiation evaluation results for the UO_2 particles coated with alumina containing a porous inner layer of alumina is given in Table 2-4.

TABLE 2-4

Evaluation of Batches 8A through 8G Which Incorporate a Porous Inner Layer of Alumina

Batch No.	Coating Thick, μ	Weight Gain, %(b)	Alpha Count Rate, cpm/gm sample		
			As-Fab.	Hot Air(b)	Thermal Cycle(c)
8A	22(a)	2.8	53.0 ± 3.3	——	——
8B	30	0.5	1.4 ± 0.7	——	——
8C	50	0.03	0.4 ± 0.5	106 ± 5	90.6 ± 4.3
8D	77	0.003	0.2 ± 0.4	51.8 ± 3.3	——
8E	106	0.04	0.8 ± 0.6	10.8 ± 1.6	6.4 ± 1.4
8F	122	0.04	0.4 ± 0.5	5.0 ± 1.2	——
8G	150	0.0003	1.0 ± 0.6	0.6 ± 0.7	3.4 ± 1.2

(a) Includes 2 micron flash coat (impermeable Al_2O_3) and 20 micron coat of porous Al_2O_3.
(b) After exposure to 1200°F air for 5 hrs.
(c) After nine cycles between 550°F and 2500°F in a reducing atmosphere.

A relatively high weight gain can be noted in batch 8A which contains a 2 micron impermeable alumina layer which probably has cracked, and a 20 micron porous layer. However, improvement can be seen in subsequent coating thicknesses. The alpha assay of the as-fabricated batches showed uniformly good quality once the first impermeable layer had been placed over the porous material (batches 8B through 8G). The hot air test showed uniformly good quality from batch 8C through 8G by the weight gain method. However, the somewhat more sensitive alpha assay technique showed a decreasing contamination with increasing coating thickness. Some surface uranium was covered by successive coating layers. In the thermal cycle test, there was some evidence of failure in batch 8C, but batches 8E and 8G showed no significant effect. In general, the batches with the thickest coatings passed all tests well. Chemical analysis of batch 8G gave a value of 42.8 w/o UO_2.

Batch 4E. Particles from this batch were used to fuel the FA-22(471E) specimen currently being irradiated in Sweep Capsule SP-5 (see Section 4.0). A 5000X electron photomicrograph of a particle from this batch was prepared in order to study the structure of the coating in more detail. Fig. 2-5 shows a 500X view of a whole particle and a 5000X view of a small section of the alumina-UO_2 interface. The dark band in the coating is now believed to be a porous alumina region which was inadvertently deposited during the

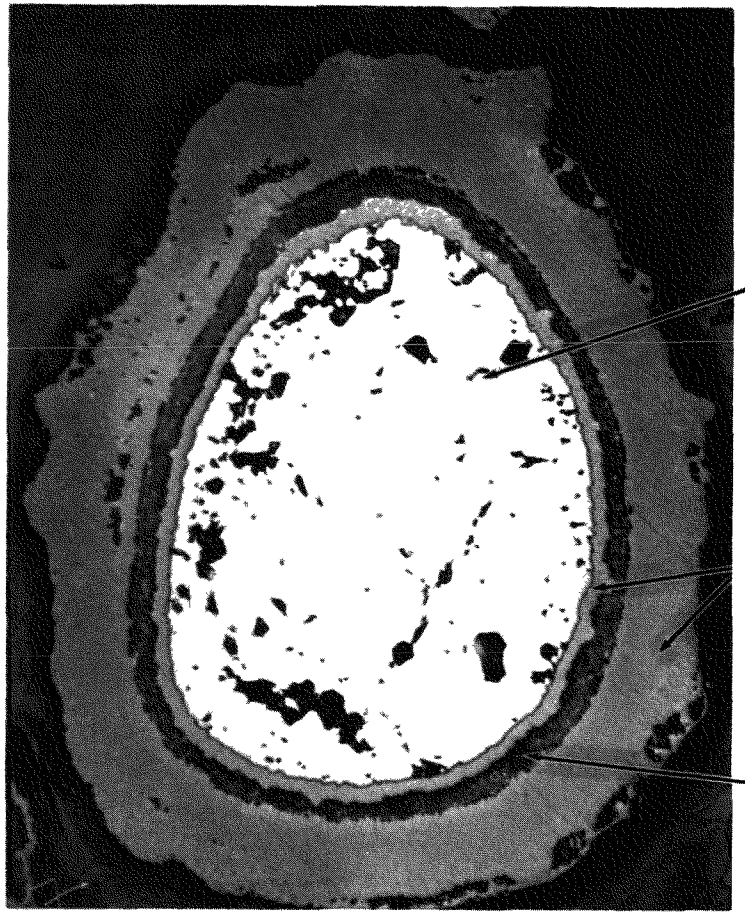

Al_2O_3 coated UO_2 particle from Batch 4E (500X).

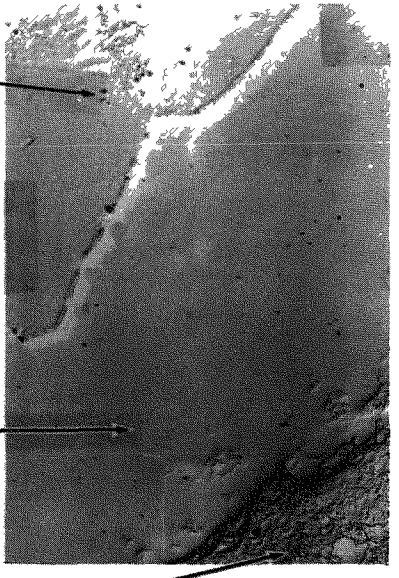

5000X magnification at Al_2O_3-UO_2 interface. Unetched.

Fig. 2-5

fabrication of this batch. In the 5000X view, the dense and continuous band of impermeable alumina can be noted between the UO_2 and the porous alumina. Grain boundaries can be clearly noted in the UO_2. The absence of any such boundaries in the alumina phase is the major reason why this type of coating has shown such good fission product retention.

Compression Test. The effect on particle coating integrity due to crushing of a graphite sphere fueled with coated particles was measured. Portions of a specimen which had previously been broken into several pieces were checked for uranium contamination by alpha assay. The particles in this specimen were coated with sintered alumina by a process which had been under study prior to development of the vapor deposition process. (3) The particles were somewhat larger than the vapor deposited alumina coated particles presently being studied, being of the order of 1000 microns diameter and 300 microns thick coatings. Portions of the fractured surfaces were alpha assayed. The count rates were found to be 0.6 ± 0.5, 0.2 ± 0.4, and 1.2 ± 0.7 cpm. This low alpha count indicates that no damage occured to these thick particle coatings. It is planned to repeat this test on spheres fueled with vapor deposited alumina coated particles.

Reaction With Graphite. The examination of several types of alumina coated UO_2 heated in graphite at 2500°F for periods of 168, 500, and 1000 hrs were completed this quarter. The three types of samples which were tested are described in Table 2-5.

TABLE 2-5

Samples Used in Carburization Test

Sample Type No.	Particle Batch No.	Graphite Filler	Pitch Binder	Max. Bake Temp., °F
1	1B	AGOT	Barrett	1700
2(a)	1B	2301	Coal Tar	2300
3(a)	2A	2301	Coal Tar	2300

(a) Pieces from an FA-22 fuel element.

In all three heating runs, a deposit formed on the inside walls of the furnace tube. The deposits consisted of alumina, silicon carbide, aluminum nitride, and/or iron silicide in addition to an unidentified phase. It is

believed that the silicon and the alumina came from the Mullite insulation tube, the iron from the graphite, and nitrogen from the furnace atmosphere. The unidentified phase was found on both the furnace walls and the specimen surfaces.

Typical results of this test are shown in Figures 2-6 through 2-15. Table 2-6 lists the sample number and heating time for each of these figures.

TABLE 2-6

List of Figures Showing Results of Graphite-Alumina Reaction Test

Figure No.	Sample Type No.	Heating Time at 2500°F	Location of Particle in the Sample
2-6	Type 1	none	——
2-7	"	168 hrs.	surface
2-8	Type 2	none	——
2-9	"	168 hrs.	center
2-10	"	500 hrs.	center
2-11	"	500 hrs.	surface
2-12	Type 3	none	——
2-13	"	500 hrs.	center
2-14	"	1000 hrs.	center
2-15	"	1000 hrs.	surface

No effect can be noted on the particle coatings in the as-fabricated condition except that some of the coatings in the Type 1 sample are cracked which undoubtedly influenced some of the results obtained for this type. After 168 hrs, several particles in Type 1 were attacked (see Figure 2-7); and there was essentially no attack to Type 2 (see Figure 2-9) and Type 3. After 500 hrs the coatings in Type 1 were completely destroyed; some thinning of the coatings in Type 2 was noted (see Figure 2-10); and some attack was beginning to occur to the Type 3 coatings (see Figure 2-13). Figure 2-11 is a view of the 500 hr. test on Type 2 except the particle shown was near the edge of the sample rather than at the center of the sample as in Figure 2-10. The coating is completely gone in Figure 2-11 which indicates a much greater reaction on particle coatings near the sample surface. The bright regions in the remaining fuel particle in Figure 2-11 are unidentified metallic appearing phases, possibly containing aluminum, which were also noted in the Type 1 fuel particle. After 1000 hrs, the particles in Type 1 were almost completely converted to a metallic phase;

and the coatings in Type 2 were almost entirely destroyed, with greater attack being noted at the edge of the sample. Coatings near the center of Type 3 samples were generally intact although there was some deterioration of the alumina (see Figure 2-14). Near the surface of the sample, complete coating attack was again noted (see Figure 2-15). It is possible that the spurious deposits noted in the furnace tube were responsible for accelerating the attack on particle coatings near the surfaces of the graphite samples.

Previous tests using sintered alumina in graphite had shown no reaction at 2500°F with graphites using coal tar pitch binders and severe reaction when resin binders were used. In the present tests, the resin binder material (Type 1) again showed the greatest degree of attack. However, the initial crackings in the coatings of Type 1 and the thin coatings of both types 1 and 2 could have been factors in the more rapid deterioration of these coatings by early exposure of the UO_2 particles. Since there was some evidence of attack even in the thickest alumina coating in graphite having a coal tar pitch binder, the maximum safe temperature must be below 2500°F and will be established by further tests.

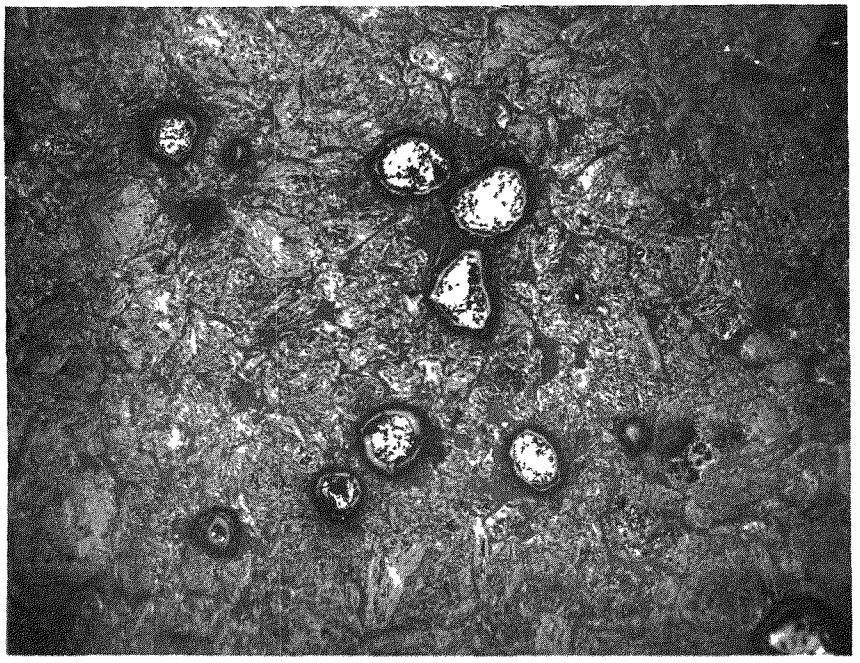

Fig. 2-6. Graphite-Al_2O_3 Specimen Type 1, as fabricated (50X).

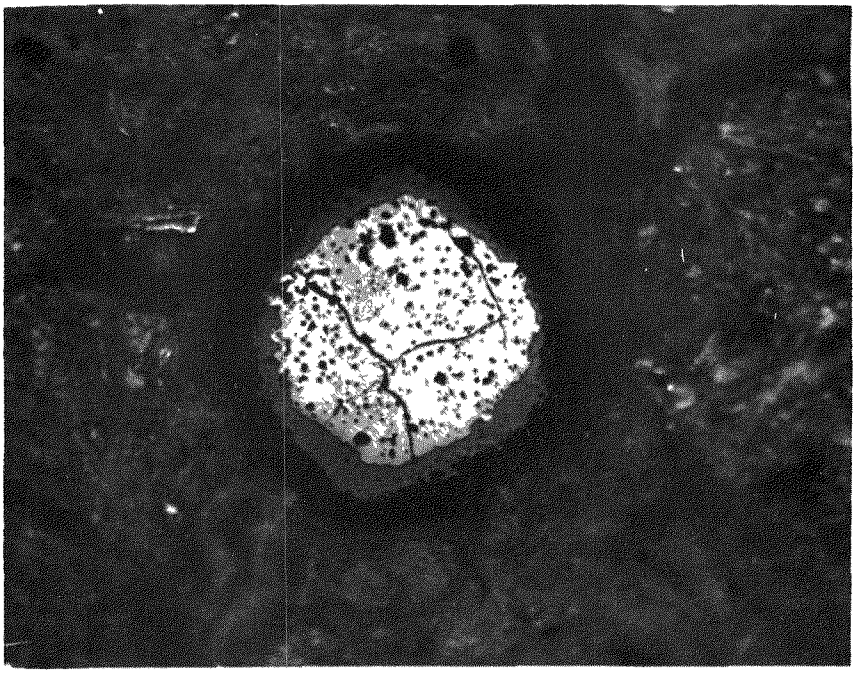

Fig. 2-7. Graphite-Al_2O_3 Specimen Type 1, after 168 hrs at 2500°F (250X).

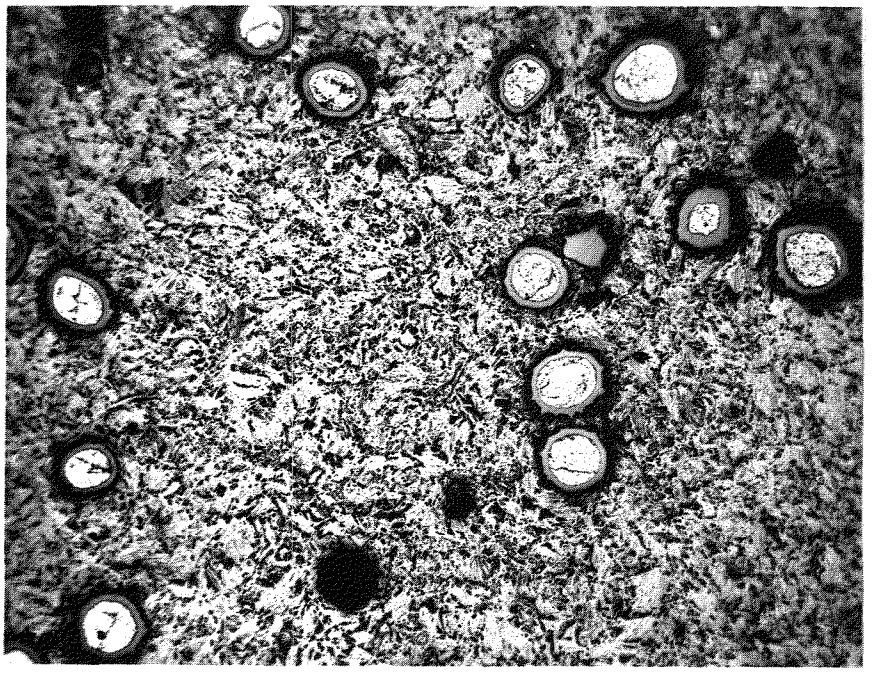

Fig. 2-8. Graphite-Al_2O_3 Specimen Type 2, as fabricated (50X).

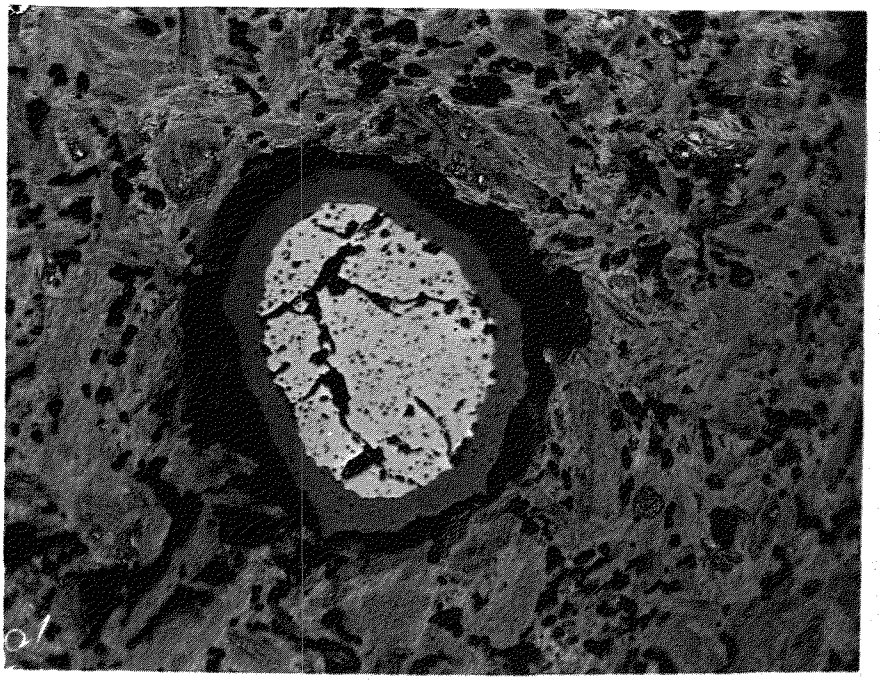

Fig. 2-9. Graphite-Al_2O_3 Specimen Type 2, after 168 hrs at 2500°F. View at center of specimen (250X).

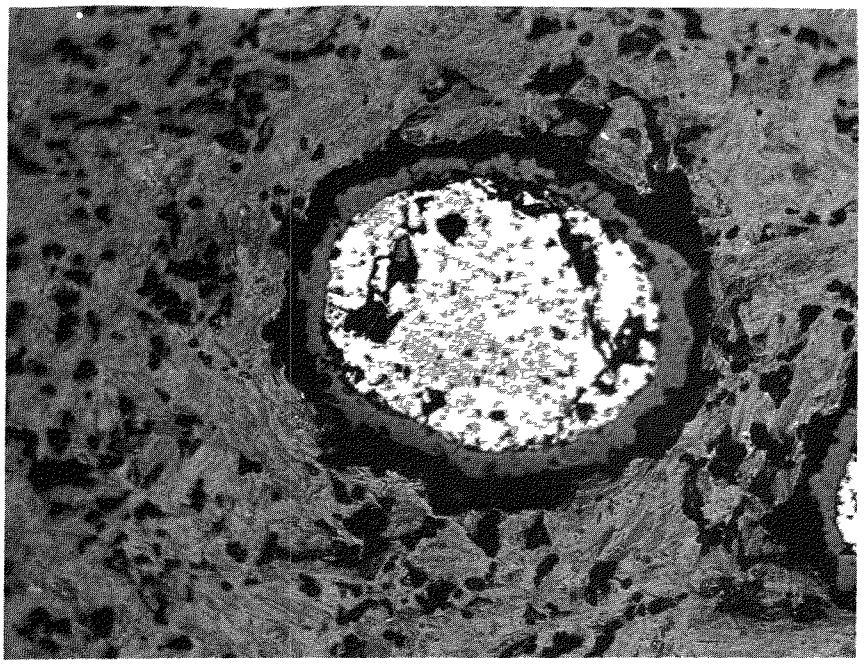

Fig. 2-10. Graphite-Al_2O_3 Specimen Type 2, after 500 hrs at 2500°F. View at center of specimen (250X).

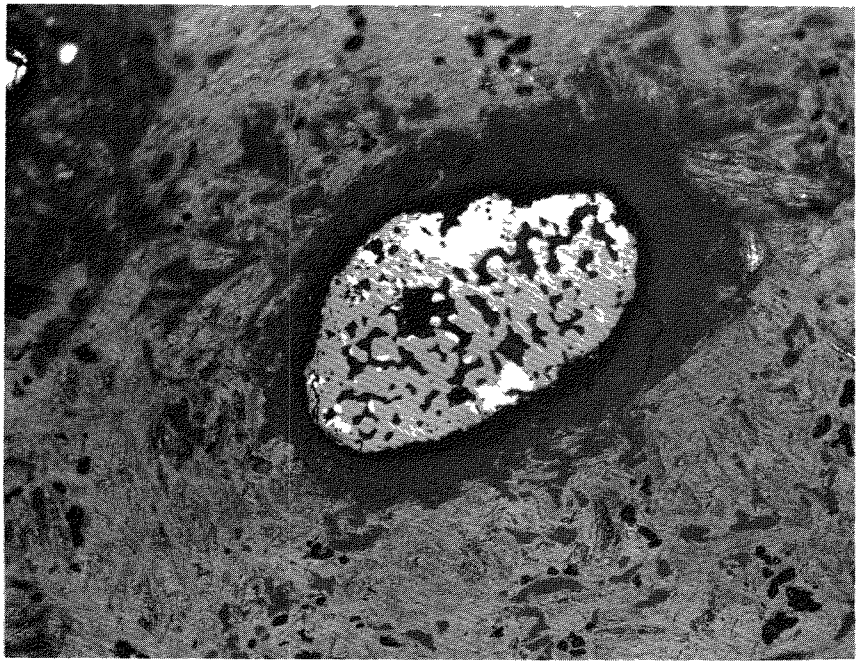

Fig. 2-11. Graphite-Al_2O_3 Specimen Type 2, after 500 hrs at 2500°F. View near surface of specimen (250X).

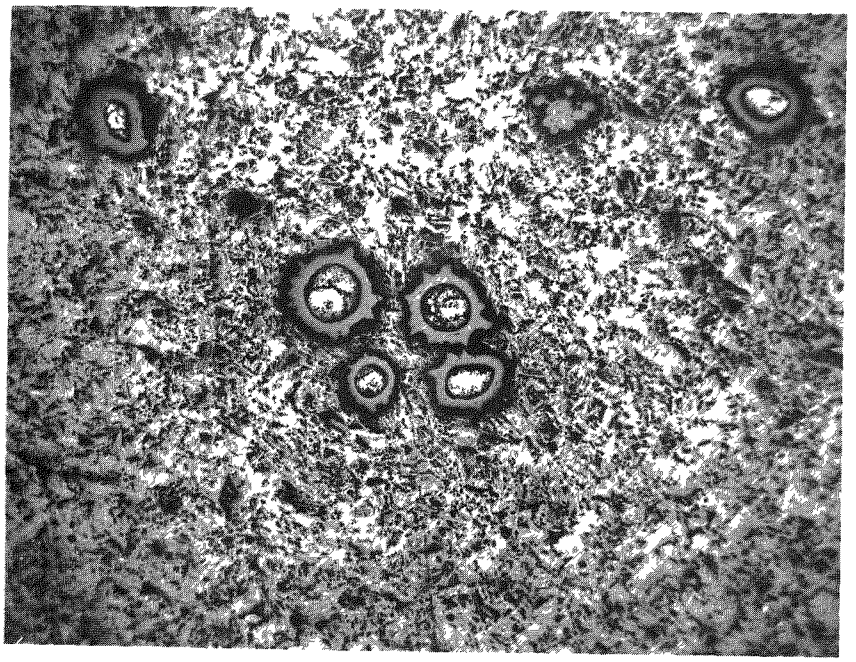

Fig. 2-12. Graphite-Al_2O_3 Specimen Type 3, as fabricated (50X).

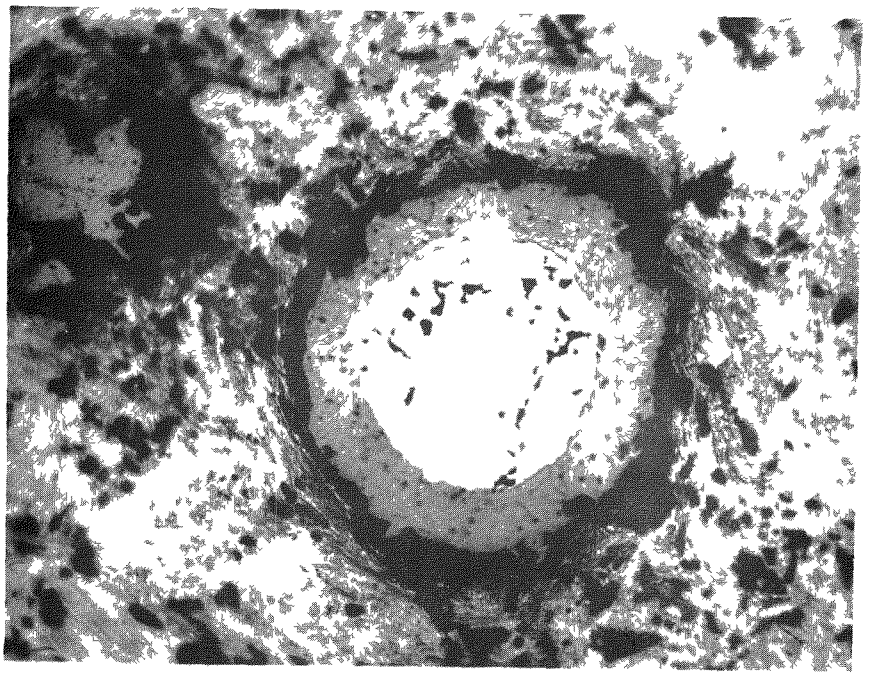

Fig. 2-13. Graphite-Al_2O_3 Specimen Type 3, after 500 hrs at 2500°F. View at center of specimen (250X).

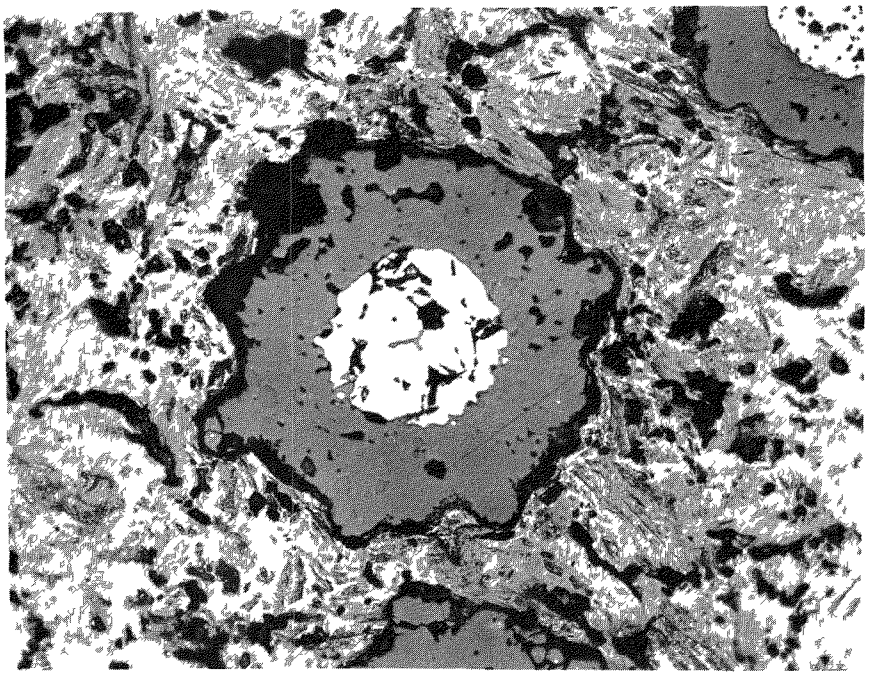

Fig. 2-14. Graphite-Al_2O_3 Specimen Type 3, after 1000 hrs at 2500°F. View at center of specimen (250X).

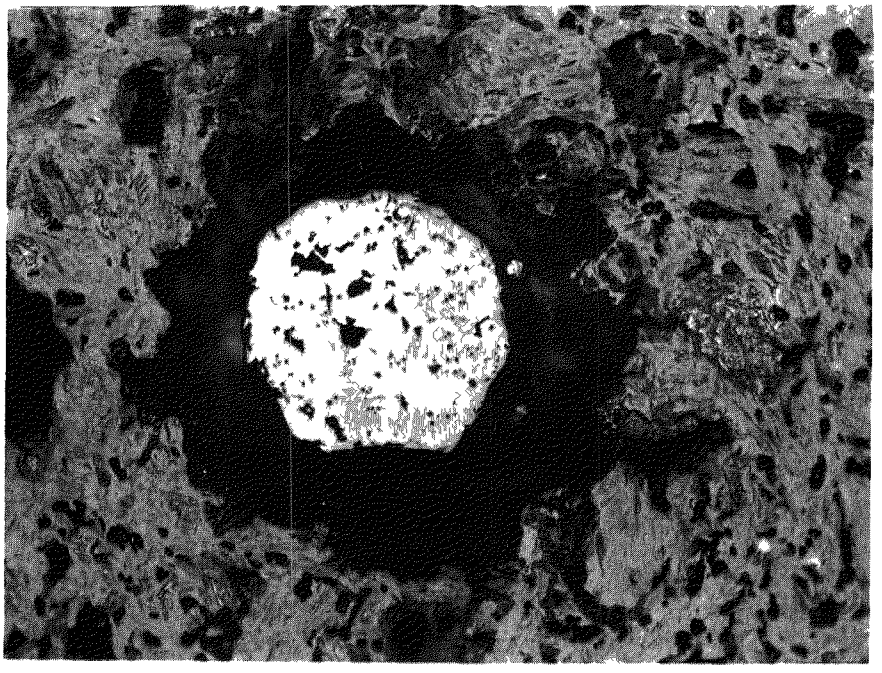

Fig. 2-15. Graphite-Al_2O_3 Specimen Type 3, after 1000 hrs at 2500°F. View near surface of specimen (250X).

3.0 Pyrolytic Carbon Coated Fuel Particles

Interest in pyrolytic carbon (Pyro C) fuel particles stems from previous experience with low permeability Pyro C coatings on the surface of PBR fuel element specimens (5). Furthermore, the use of a Pyro C coating on fuel particles would remove the temperature limitations imposed by the chemical reaction between metal oxide particle coatings and the graphite matrix and would not effectively displace moderating material when dispersed in graphite.

An exploratory program on Pyro C coatings on UC_2 particles was continued at the Battelle Memorial Institute during this quarter. The basic process consists of fluidizing a bed of UC_2 particles in a helium stream containing a hydrocarbon gas such as methane or acetylene. The fludized bed is externally heated which causes the hydrocarbon gas to decompose and deposit carbon on the UC_2 particle surfaces (7).

During the previous quarter, UC_2 particles were coated at deposition temperatures of 1800 to 2000°F. The UC_2 particles used in these batches were irregular in shape and there was some evidence of cracking at sharp corners. When additional coating layers were applied to Pyro C coated particles, the coating interfaces were readily apparaent in contrast to the lack of visible boundaries between adjacent alumina coatings. The pyrolytic carbon as deposited on the particles appeared dense and impermeable. However, when the particles were heated above the coating deposition temperature, coatings were found to crack due to the higher expansion coefficient of the UC_2 particle.

During this quarter, additional evaluation was performed on these particles, several graphite spheres fueled with these particles were prepared, and spherical UC_2 shot was coated at a higher temperature.

3.1 Fabrication of Pyrolytic Carbon Coated Fuel Particles

Batches PyC-1 and PyC-2 which were made during the previous quarter were limited in coating thickness by carbon soot formation which tended to plug the discharge lines from the reaction vessel. Several attempts were made to eliminate this problem by introducing CO_2 to react with the excess carbon but no significant effect was found.

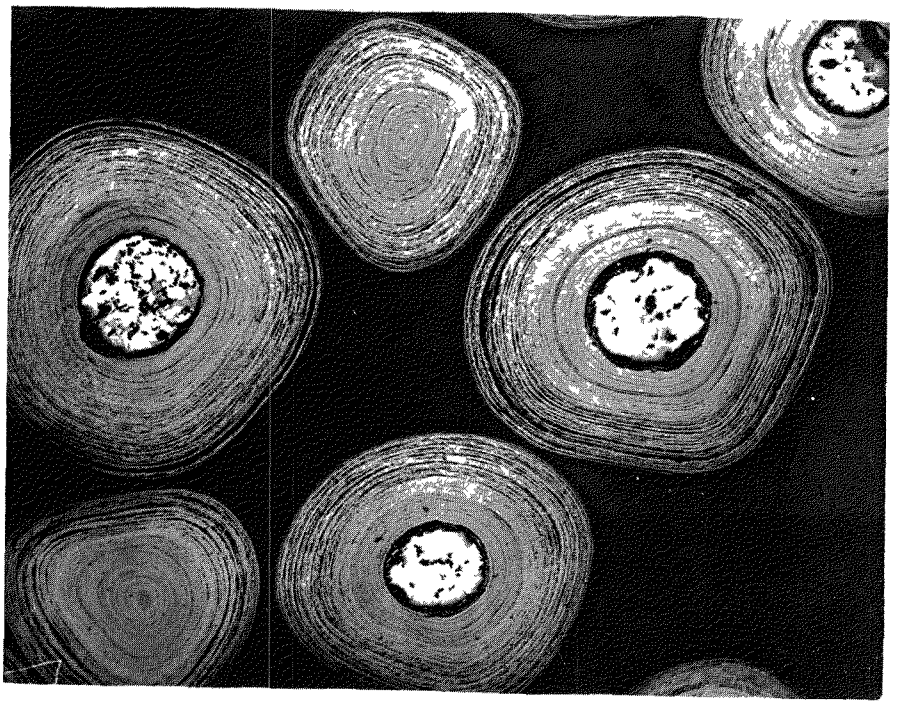

Fig. 3-1. Batch PyC-5 showing 160 micron pyrolytic carbon coatings on UC_2 (80X).

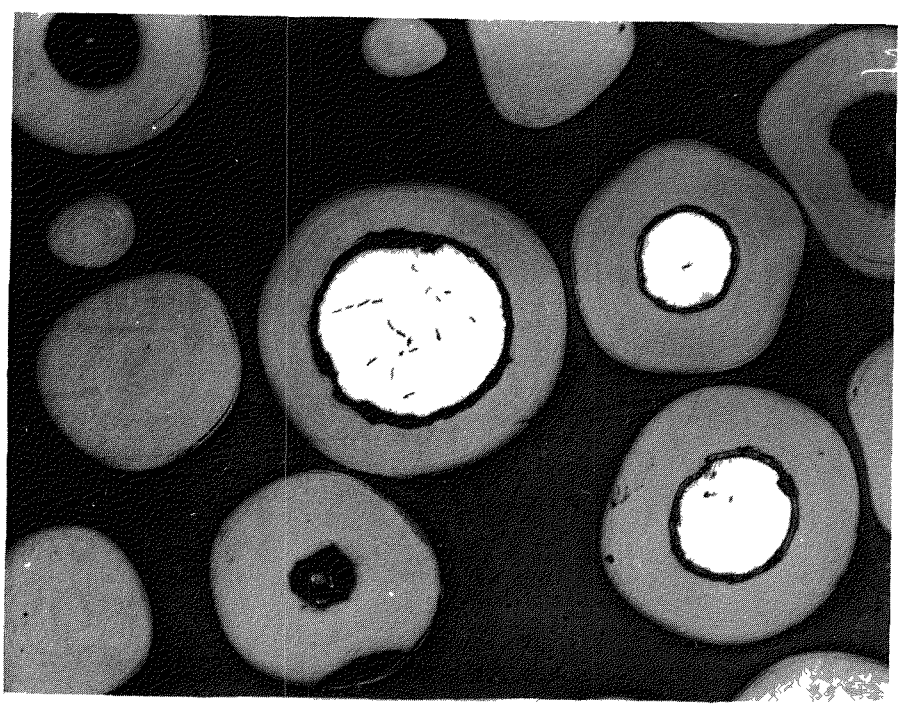

Fig. 3-2. Batch PyC-6 showing 80 micron pyrolytic carbon coatings on UC_2 (100X).

3.2 Evaluation of Pyrolytic Coated Fuel Particles

The procedures used to evaluate pyrolytic carbon coated particles were generally similar to those used for alumina coated particles except that a nitric acid leach test was used to determine coating integrity rather than the hot air oxidation test.

The leach test is performed by immersing the coated particles in a hot nitric acid solution for several hours and analyzing the leach solution. In the cases of both batches PyC-5 and PyC-6 as-fabricated, the amount of uranium found in the leach solution was equal to or less than the detection limit of 10^{-3}% of the uranium contained in the particles indicating excellent coating integrity. The uranium content of these batches were found by chemical analysis to be 22.9 w/o and 53.8 w/o respectively for batches PyC-5 and PyC-6.

Because of an interest in using this type of pyrolytic carbon coating as a reaction barrier between the fuel particles and a silicon carbide coating which could be applied to the outer surface of a fueled graphite sphere, thermal cycle tests were performed on these particles to 3600°F in an argon atmosphere. Three such cycles were performed on each batch with the particles being allowed to cool to room temperature after each heating cycle while in the furnace. The results of this test are given in Table 3-2 where alpha assays before and after thermal cycling are compared.

TABLE 3-2

Thermal Cycle Test Results on Batches PyC-5 & PyC-6

Batch No.	Condition	Net Alpha Count Rate, cpm/gm sample	Equivalent Uranium, mg/gm sample
PyC-5	As-Fab.	1.9 ± 1.3	.0026
PyC-5	After TC.	21.4 ± 3.7	.030
PyC-6	As-Fab.	1.9 ± 1.3	.0026
PyC-6	After TC.	65.6 ± 5.2	.088

Previous thermal cycle test results on batches PyC-1 and PyC-2 under similar conditions which had coatings applied at only 2000°F showed a 3 order of magnitude increase in exposed uranium. This increase is significantly lower for batches PyC-5 and PyC-6 which were fabricated at 2450°F and had thicker coatings. A leach test on batch PyC-5 after thermal cycle indicated that 0.6% of the particles had cracked, on the assumption that all uranium was leached from cracked particles. Thus, the

safe upper limit for this type of Pyro C coated UC_2 will still be somewhat below 3600°F.

During this quarter, fission product retention tests were completed on particles from batch PyC-1 and on a graphite sphere fueled with these particles. These materials were subjected to the neutron activation test which consists of a short neutron irradiation followed by heating in a laboratory furnace. The escape of Xe 133 as function of heating time and temperature can be measured. The results are shown in Table 3-3.

TABLE 3-3.

Neutron Activation Tests on Batch PyC-1.

	Test Temp, °F	Time, Min.	Fractional Release of Xe 133
A. Particles only	1600	160	$<4.5 \times 10^{-6}$ (a)
	2000	93	$<4.5 \times 10^{-6}$ (a)
	2400	65	4.7×10^{-4}
B. Particles in Graphite Sphere	1000	30	1.7×10^{-3}
	1700	30	3.4×10^{-4}
	2100	65	6.8×10^{-4}
	2500	35	1.5×10^{-3}
	2700	15	4.9×10^{-4}

(a) Limit of detection.

The results on the particles show that up to 2000°F (i.e. the coating deposition temperature), the pyrolytic carbon coating exhibits excellent fission product retention. At 2400°F, the sudden increase in Xe 133 release indicates that some of the particle coatings have cracked which confirms the results from previous thermal cycle tests. The results on the graphite sphere fueled with Pyro C coated particles indicates that the coatings have undergone some damage during either the mixing, molding, and/or baking operations of sphere fabrication. Actually, an alpha assay of the sphere surface prior to neutron activation test indicated a surface uranium concentration of about 0.09 mg of uranium which is 1.9×10^{-3}% of the total uranium in the sphere. Thus it appears that uranium contamination must have been spread throughout the entire sphere.

During the next quarter, it is planned to test fission product retention of particles from batch PyC-6 and to explore pyrolytic carbon particle coatings at temperatures higher than 2450°F.

4.0 Irradiation Testing

The major irradiation test conducted during this quarter was the continuation of the Capsule SP-5 irradiation in the Battelle Research Reactor. The design of this capsule has been described in the previous Quarterly Report (5). Briefly, the capsule consists of two sections. The top section is divided into two compartments, one containing an FA-22 specimen (fueled with alumina coated UO_2) and the other an FA-23 specimen (coated with Si-SiC). Each compartment has helium inlet and outlet lines to permit measurement of fission product leakage rates in a gas analysis train located on the floor above the BRR pool. The bottom section of the capsule contains 4 specimens in a common compartment with no provision for measuring fission product leakage. These specimens are one additional FA-22 and FA-23 together with two FA-20 specimens (pyrolytic carbon surface coating). All six specimens are full-scale PBR fuel elements, 1-1/2 inches in diameter, and loaded with 4.75 gms of highly enriched uranium. Specimen temperature is a function of the thermal resistance of the capsule parts and the nuclear heat generation rate. Specimen temperatures and heat generation rates are calculated from data obtained from thermocouples located in special graphite blocks used to hold the specimen within the capsule.

Irradiation of Capsule SP-5 was started on April 6, 1960. Normal operation continued through the present quarter and is scheduled to continue through the next quarter. Typical operating conditions for the specimens in Capsule SP-5 which prevailed throughout this quarter are given in Table 4-1.

TABLE 4-1

Operating Conditions for Capsule SP-5 Specimens

Specimen No.	Measured Block Temp. °F	Heat Gen. Rate, KW	Calc. Surface Temp., °F	Calc. Central Temp., °F
Sweep:				
FA-22(471E)	1090	1.5	1360	1550
FA-23(E8-7)	1010	1.6	1300	1440
Static:				
FA-22(470E)	——	1.4	1360	1540
FA-20(338E)	——	1.3	1360	1460
FA-23(E8-12)	——	1.0	1300	1390
FA-20(345E)	——	0.8	1360	1420

Another type of irradiation test which has been used in the PBR Fuel Element Program is called the Furnace Capsule test. In this test, fission product leakage can be continuously measured while a specimen is under low level irradiation. Specimen temperatures are controlled by an electric heater. Furnace Capsule SPF-3 containing an FA-22 specimen had been started during the previous quarter while using the off-gas train now in use on Capsule SP-5. A new off-gas train for Furnace Capsule operation was constructed during this quarter. Additional data from Capsule SPF-3 will be obtained during the next quarter.

4.1 Data for Alumina Coated UO_2 Fueled Specimen (FA-22).

The FA-22 specimens in Capsule SP-5 were fueled with alumina coated UO_2 particles from batch 4E (see Table 2-1) which were made by Battelle. The particles were incorporated in graphite by the National Carbon Co. After mixing, molding and baking, no further treatment was given to the spheres. No attempt was made to minimize or remove molding bands in order not to disrupt the fuel particle coatings. Pre-irradiation evaluation of these spheres was described in the previous Quarterly Report (5). Briefly, an alpha assay of the as-fabricated particles from batch 4E indicated a uranium contamination on the particle surfaces of about 3×10^{-3}% of the total uranium in the particles. An alpha assay of the surface of the FA-22 (471E) specimen selected for the sweep compartment of SP-5 indicated a uranium concentration at the surface of 10^{-4}% of the uranium in the sphere.

On July 25, 1960, the eighth cycle of Capsule SP-5 irradiation in the BRR was concluded. At an average irradiation time of 10-1/2 full power days per cycle, the radiation exposure to FA-22 (471E) at this point was 3000 KWH. This exposure is equivalent to 21,600 MWD/metric ton of uranium, 1.3×10^{18} fissions/cc of specimen volume, or 3.3 a/o of U 235 atoms fissioned. During this quarter, nine samples of the off-gas stream from specimen FA-22 (471E) were taken and analyzed for fission products. Data were obtained for 5 long-lived fission product gases: Kr 85m, Kr 87, Kr 88, Xe 133 and Xe 135. Occasionally, one or more of these isotopes would be below the limits of sensitivity. Leakage factors (R/B) were calculated for each isotope by dividing the measured leakage rate by the equilibrium production rate for that isotope.

All data including three gas samples taken prior to this quarter are plotted in Figure 4-1 as R/B vs. exposure. Variations in specimen surface temperature are also shown in this figure. It can be noted that from the

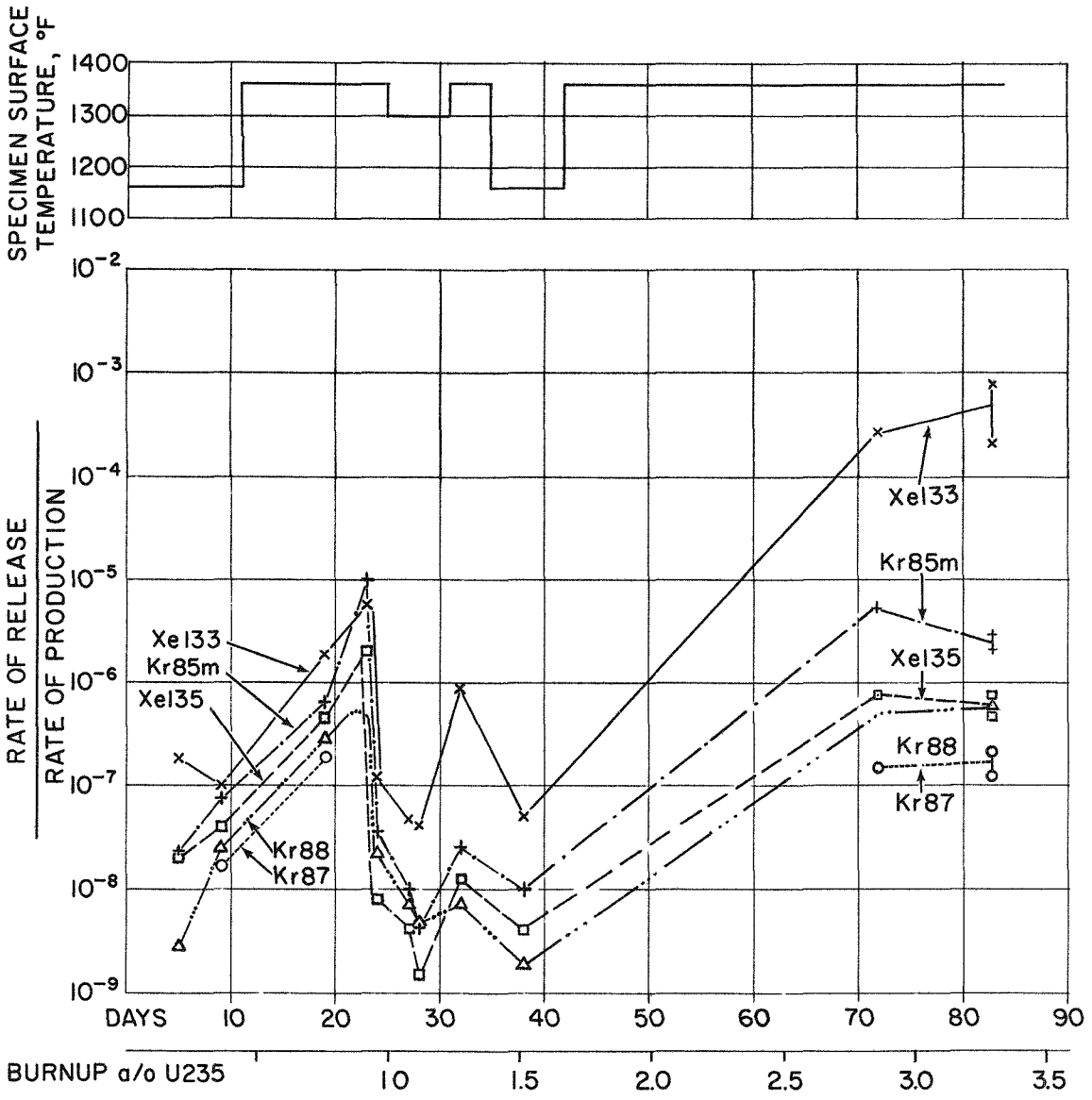

FIG. 4-1 FISSION PRODUCT RETENTION BY GRAPHITE SPHERE FUELED WITH Al_2O_3 COATED UO_2
(DATA FROM CAPSULE SP-5)

38th day to the 72nd day no data is shown. During this period, certain revisions relating to the general operation and safety features of the gas train were performed. Although there was no helium flow through the capsule, it remained under full power irradiation while the gas train was being modified. Several of the Kr 87 data points are not shown in Figure 4-1, (i.e. from about the 20th to the 40th day) since the Kr 87 leakage factors at these points were below the limit of detection which is estimated to be 10^{-9}. Occasionally, several Kr 88 readings were not obtained since the gamma peak used to identify Kr 88 was masked by high activity from other isotopes. The two sets of data points shown at the 83rd day are for two successive gas samples which were taken to check reproducibility.

Leakage factors for five other fission products were measured in a special experiment performed during this quarter. These fission products included three short-lived isotopes (3.2m Kr 89, 16s Xe 140, 1.7s Xe 141), 8d I 131 and 21h I 133. These isotopes are not normally measured in the off-gas train located above the pool since their half-life is so short, several of their non volatile daughters are only beta emitters, and/or the amount of plateout in the piping leading to the analytical trap is unknown. Consequently a special non-volatile fission product trap was used to obtain these data points. This trap consisted of a stainless steel container 2-1/2 " OD filled with layers of stainless steel mesh to a length of 40 inches. The trap was located in the BRR pool near the sweep helium outlet connection on Capsule SP-5. Transit time from the Capsule to the trap was 2 seconds and the residence time in the trap of the helium containing fission products was 90 seconds during which time non-volatile fission products and iodine deposit on the stainless steel mesh. In normal capsule operation, helium flow by-passes the non-volatiles trap.

On the 30th day of Capsule SP-5 operation, helium flow was diverted through this trap for a 48 hour period. The trap was then dismantled and subjected to a radiochemical analysis. Sr 89, Ba 140, Ce 141, I 131, I 133, Te 132 and Cs 137 were detected in the trap. Quantitative data was obtained for the first five isotopes.

Isotope concentrations were measured as a function of pad position in the trap. A few spot checks showed that less than 2% of the Sr 89, Ba 140 and Ce 141 were on the walls of the trap so that wall effects were neglected. The relative pad activities as a function of travel time through the trap were plotted in Figure 4-2 (Sr 89, Ba 140, Ce 141) and Figure 4-3 (I 131 and I 133).

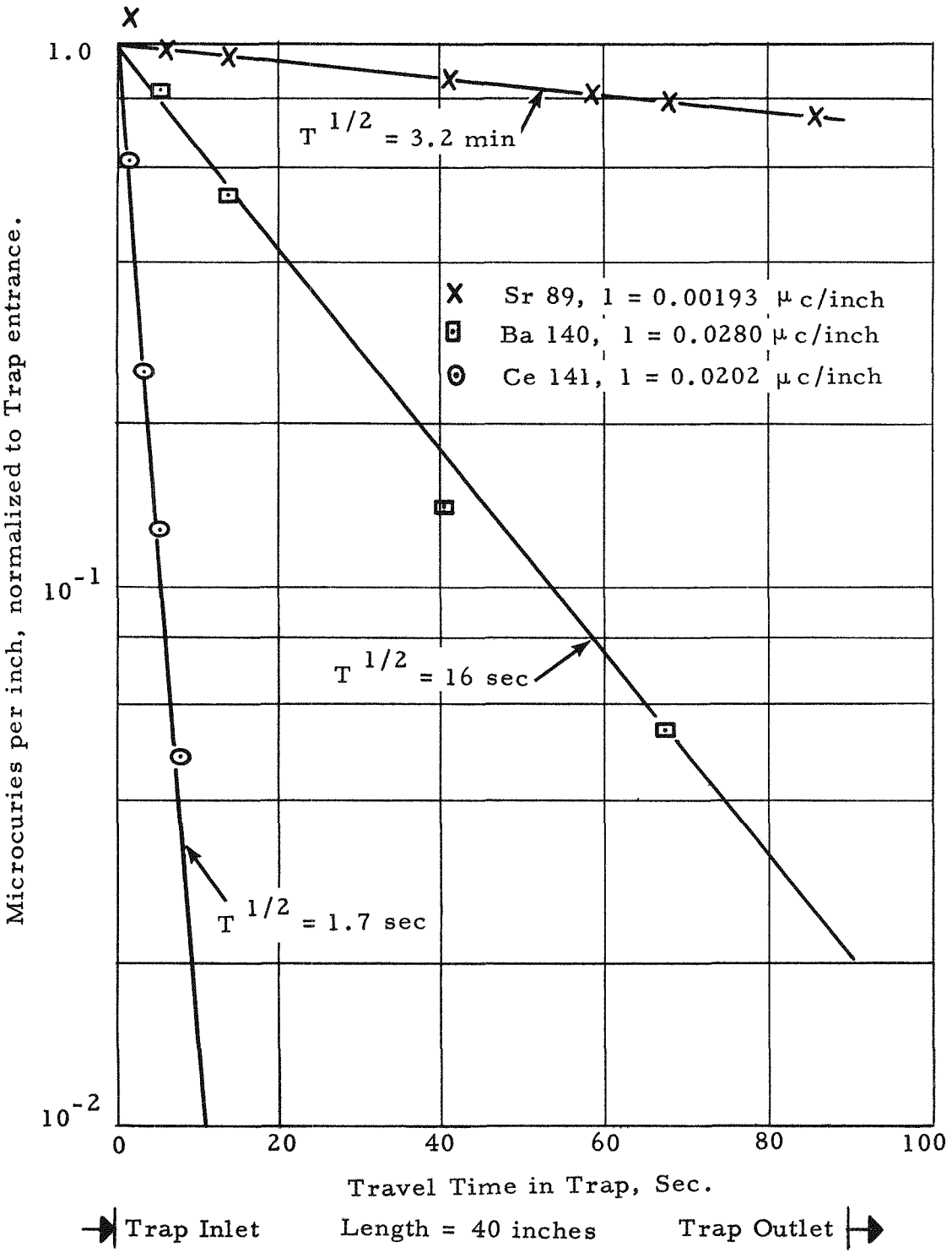

FIG. 4-2. Distribution of Sr 89, Ba 140, and Ce 141 in Non-Volatiles Trap for Specimen FA-22(471E).

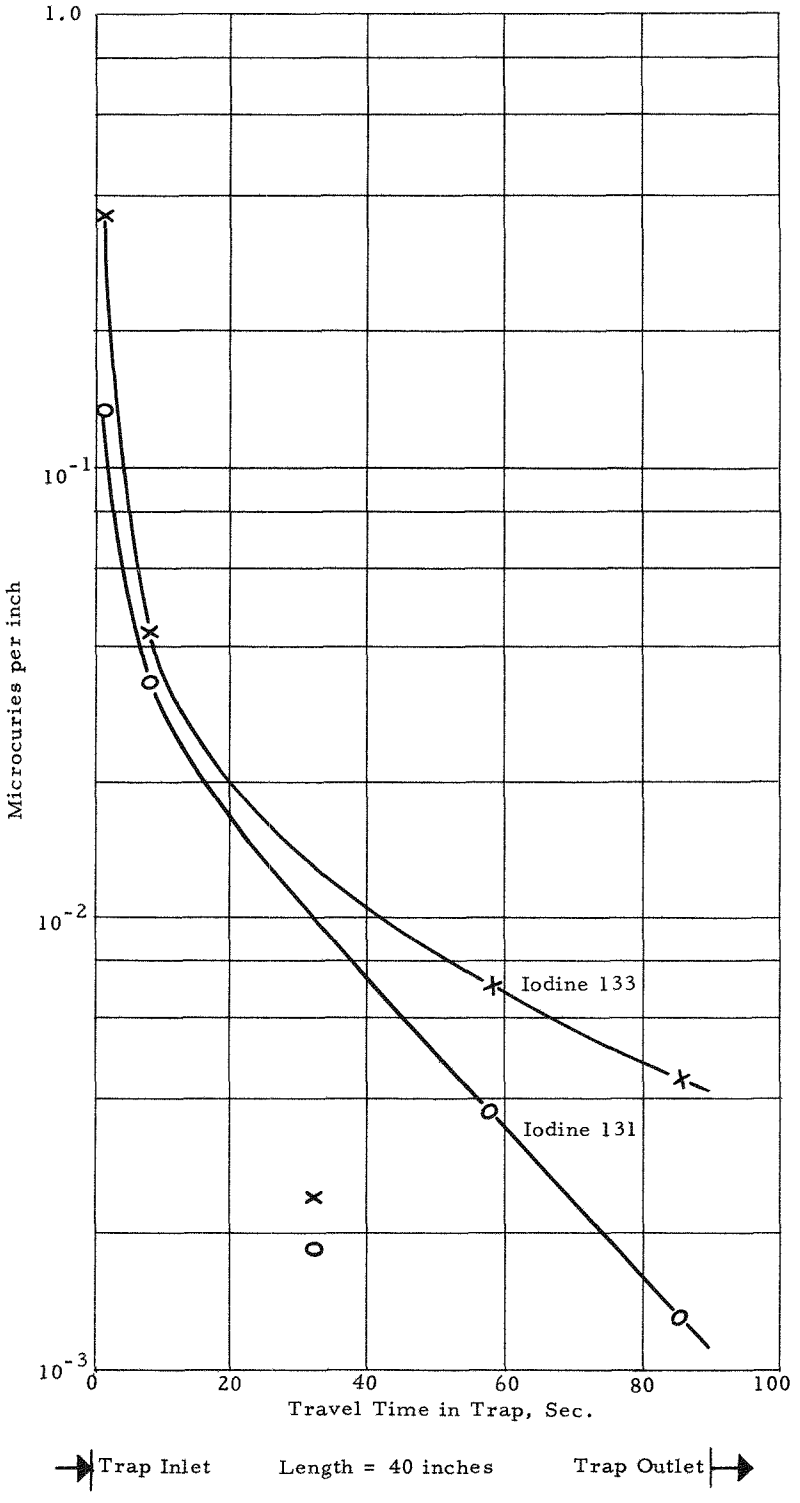

FIG. 4-3. Distribution of I 131 and I 133 in Non-Volatiles Trap for Specimen FA-22(471 E)

If it is assumed that non-volatile daughter products deposit on the stainless steel mesh immediately upon the decay of its volatile parent isotope, then the concentration of the non-volatile daughter product through the trap should be a function of the half-life of the gaseous precursor. These predicted deposition curves are also shown in Figure 4-2. As can be noted, there is excellent agreement between the theoretical curves and the actual data. Essentially all of the Ba 140 and Ce 141 was deposited in the trap. Only about 30% of the Sr 89 was deposited in the trap with the remainder passing out of the trap as undecayed Kr 89. There is practically no decay of the I 131 and I 133 during their passage through the trap. The assumption of a constant removal efficiency per inch of trap would explain the exponential nature of the iodine curves seen in Figure 4-3. Essentially all of the iodines are removed by the trap. The leakage factors summarized in Table 4-2 are based on these data. These leakage factors are of the same order of magnitude as for the other isotopes shown in Figure 4-1 at the 30th day.

TABLE 4-2

Summary of Non-Volatiles Trap Data for Specimen FA-22(471E) in Capsule SP-5

Trapped Species		Precursor		
Isotope	Half-Life	Isotope	Half-Life	Leakage Factor
Sr 89	54 day	Kr 89	3.2 min.	3.0×10^{-7}
Ba 140	12.8 day	Xe 140	16 sec.	1.1×10^{-7}
Ce 141	32 day	Xe 141	1.7 sec.	1.3×10^{-7}
I 131	8.05 day	———	———	1.2×10^{-8}
I 133	20.8 day	———	———	1.4×10^{-8}

Several interpretations can be made concerning the data shown in Figure 4-1 and Table 4-2.

1. During the early part of the irradiation, no significant dependence of leakage factor on isotope half-life can be noted. If the measured leakage had been due to a diffusion mechanism through the alumina coatings on the UO_2 particles, lower leakage rates for the short-lived isotopes should have been found because of the more rapid decay rate of these isotopes to non-volatile daughters during diffusion. Since this does not appear to be the case, it strongly suggests that the "leakage" being measured actually arises from slight amounts of uranium contamination external to the alumina coatings. The existence of some cracked coatings can be completely discounted except to note that the complete release of any isotope

from only one of the 500,000 particles in the specimen would correspond to an R/B of 2×10^{-6}.

2. Some evidence of leakage factors being dependent on temperature can be noted during the early part of the irradiation. One explanation could be the effect of temperature on diffusion through the graphite matrix.

3. The significant leakage factors found for the iodine isotopes indicate that all leakage factors for the xenons must include contributions from the direct leakage of xenon as well as from iodine which leaked from the specimen, deposited on a convenient surface, and subsequently decayed to xenon.

4. During the latter part of the irradiation, an increase in leakage factor for Xe 133 and Kr 85m is noted in relation to the leakage factors for the relatively shorter-lived Kr 87 and Kr 88. This spectrum of leakage factors could be indicative of measurable diffusion through the alumina coatings starting to occur. This could be due to either a saturation effect in the alumina or else neutron damage has begun to affect the permeability of the alumina. Data from the next non-volatile trap which is scheduled to be operated during the next quarter should add further to the evaluation of this point.

4.2 Data for Si-SiC Coated Specimen (FA-23).

The FA-23 specimens in Capsule SP-5 consist of a fueled graphite sphere 1-1/4" in diameter surrounded by an unfueled graphite shell 1/8" thick. The outer surface of this sphere is coated with a .003" thick layer of siliconized silicon carbide (Si-SiC).

As described in the last Quarterly Report (5), the fission product release rates from this specimen were found to be extremely low during the first two cycles of operation. However, as the specimens were brought up to power at the beginning of the third cycle, a sharp rise in fission product release was noted. A summary of the long-lived volatile fission product release data is given in Table 4-3.

TABLE 4-3

Summary of Long-Lived Volatile Fission Product Release Data from Specimen FA-23(E8-7) in Capsule SP-5.

Sample No.	Days of Irradiation	R/B, (Rate of Release/Rate of Production) Kr 85m	Kr 87	Kr 88	Xe 133	Xe 135
1	11	Nil	Nil	Nil	Nil	Nil
2	12	Nil	Nil	Nil	Nil	Nil
3	16-17[a]	2.6×10^{-9}	Nil	1.5×10^{-9}	5.7×10^{-9}	1.5×10^{-9}
4	21	(b)	(b)	(b)	7.9×10^{-3}	(b)
5	21	6.6×10^{-4}	2.0×10^{-3}	1.7×10^{-4}	3.0×10^{-3}	1.1×10^{-4}
6	21	3.8×10^{-3}	1.2×10^{-4}	6.6×10^{-4}	6.3×10^{-3}	9.3×10^{-4}
7	32	3.8×10^{-4}	1.3×10^{-4}	2.0×10^{-4}	5.2×10^{-4}	1.0×10^{-4}

(a) Sample collected over 22 hour period (rather than 2 hour period) because of low release rate.

(b) These species decayed out during long cooling period necessitated by high activity in this sample.

Sample No. 4 was taken just after Capsule SP-5 was brought up to power for the third cycle. Just prior to startup, gas flow throught the compartment containing the FA-23(E8-7) specimen showed no evidence of high fission product leakage. It is therefore assumed that whatever the type of coating failure which caused the large increase in leakage factor, it was associated with the increase in internal temperature gradient as the specimen came up to power. The exact nature of the coating failure will not be known until Capsule SP-5 is opened in the Hot Cell for examination.

No further gas samples were taken for the purpose of measuring long-lived fission product release. The helium inlet and outlet valves for the FA-23(E8-7) specimen were shut off. During the day of irradiation when the large increase in fission activity was first noticed, a non-volatile fission product trap was put on-stream for a two hour period. The procedures used were similar to those used for the non-volatiles trap experiment with the FA-22 specimen described in Section 4-1 except that the helium transit time through the trap was 125 seconds.

Due to the long delay time betweem sampling and the radiochemical analysis, no iodine activity was found. Isotopes which were detected include Sr 89, Ba 140, Ce 141 and Cs 137. Plots of isotope concentration as a function of travel time through the trap again showed excellent agreement with the theoretical prediction based on the half-lives of the volatile precursors. The leakage factors shown in Table 4-4 were calculated from these data.

TABLE 4-4

Summary of Short-Lived Volatile Fission Product Release Data from Specimen FA-23(E8-7) in Capsule SP-5.

Note: Sample taken during 21st day of irradiation

Trap Species	Precursor		
	Species	Half-Life	R/B
Cs 137	Xe 137	3.9 min.	4.0×10^{-4}
Sr 89	Kr 89	3.2 min.	7.2×10^{-4}
Ba 140	Xe 140	16 sec.	3.4×10^{-5}
Ce 141	Xe 141	1.7 sec.	4.6×10^{-6}

The leakage factors in Table 4-4 are in rather good agreement with the long-lived fission product leakage factors on the 21st day shown in Table 4-3. A trend to smaller leakage factors with shorter half-life can be noted in Table 4-4. This indicates some sort of delay in the escape of these fission products which causes a greater fraction of the shorter-lived fission products to decay within the sphere thus preventing further escape of their non-volatile daughters. If it is assumed that there is a fault in only the Si-SiC coating in this specimen, then the 1/8" unfueled graphite shell on this specimen could be the primary diffusion barrier which is retarding the escape of the shorter-lived volatile fission products.

5.0 Natural Graphite

An inherent characteristic of the Pebble Bed Reactor concept is the fixed 39% voidage in the ball bed region. One method of increasing the amount of carbon moderator in a Pebble Bed core to account for this high voidage is to replace some of the spheres with solid graphite posts. This increases the amount of carbon in the core but at the same time decreases the amount of heat transfer surface in the core. Another method of increasing the amount of carbon moderator is to increase the graphite density of the fueled spheres. For example, in the reference design for the 125 eMW-PBR (2), a graphite density of 1.68 g/cc was used and it was found necessary to replace 25% of the core volume with solid graphite posts to achieve the optimum conditions for that plant. The same effective carbon loading could have been achieved if 2.1 g/cc graphite spheres were used with no fixed graphite posts, thus increasing the thermal capacity by about 33% for the same total core size.

The general method of achieving high density graphite is by successive carbonaceous reimpregnations and regraphitizations of the graphite body. Densities up to about 1.9 g/cc have been achieved by this technique. Another method is the use of suitable starting materials which can be molded and baked to directly form a high density graphite body in only one step. One such material is natural graphite powder.

An exploratory program on the fabrication of graphite bodies using natural graphite as the filler material was continued at the Battelle Memorial Institute during this quarter. Densities in excess of 2.0 g/cc had been achieved using natural graphite powder with no binder. However, these bodies had little strength. One of the major objectives of the program was to determine whether suitable strength characteristics could be achieved by the addition of a binder without a serious decrease in density. During this quarter, a variety of natural graphites, binders, and binder contents were explored.

Three types of purified natural graphite powder were obtained from the Charles Pettinos Graphite Corp. as described in Table 5-1.

TABLE 5-1

Natural Graphite Materials

Grade No.		Impurities	Particle Size
138	Mexican, amorphous	0.9%	99%, -325 mesh
6387	Madagascar, crystalline	0.1% (B < 1 ppm)	100%, - 200 mesh, avg. particle size, ~ 10.6 μ
6405	Madagascar, crystalline	0.1%	0.03%, +100 mesh 2.03%, -100, +200 mesh 17.98%, -200, +325 mesh 79.96%, -325 mesh.

A series of 1/2" x 1/2" cylindrical pellets were prepared using the three types of natural graphite shown in Table 5-1. Four types of binder were used, including two types of phenolic resin, a coal tar pitch, and furfural alcohol. Binder content ranged from 0 to 40 gms per 100 gms of natural graphite. After mixing, the pellets were cold pressed, cured at 400°F, prebaked in vacuum at 1500°F, and finally baked at 2500°F in argon. Density measurements were taken at each stage of fabrication and crushing strengths of the finished pellets were measured. A summary of the results is given in Table 5-2.

Several trends can be noted in Table 5-2. Lower densities result with a high binder content. Lowest densities resulted with coal tar pitch binder. The strengths of the resin bound pellets were generally higher than for the pitch bound pellets. For comparison purposes, two 1/2" x 1/2" cylinders were machined from AGOT graphite of 1.70 g/cc density. The compressive strengths for these pieces were found to be 3,139 psi and 3,445 psi.

The highest densities were achieved with the 6405 and 6387 graphites with the lower BV1600 binder contents. Consequently an additional series of pellets were prepared to explore this range in somewhat more detail. The use of thermax carbon black was also investigated using the same fabrication and test procedures used for the pellets in Table 5-2. The results are shown in Table 5-3.

TABLE 5-2

Density and Strength of Natural Graphite Pellets (1st Series)

Graphite Composition [a]	Gms. binder per 100 gms of filler	Green Density, g/cc [b]	Baked Density, g/cc [c]	Compressive Strength psi [c]
6387-none	none	2.14	1.95[b]	1,000[d]
6387-BV1600	20	2.00	1.92	5,000
6387-BV1600	35	1.66	1.55	4,700
6387-BV1600	50	1.74	1.77	5,200
6387-pitch	30	1.87	1.60	3,900
6387-pitch	35	1.86	1.49	3,200
6387-pitch	40	1.81	1.45	2,700
6387-79L	20	1.91	1.85	3,800
6387-79L	30	1.78	1.67	2,500
6387-FA	40	1.72	1.68	2,600
6405-none	none	2.03[c]	2.06	1,900
6405-BV1600	20	2.02	2.02	2,900
6405-BV1600	35	1.93	1.93	3,400
6405-BV1600	50	1.89	1.88	3,400
6405-pitch	30	1.90	1.60	2,400
6405-pitch	35	1.89	1.63	3,300
6405-pitch	40	1.86	1.57	3,000
138-none	none	1.71[c]	1.72	2,400
138-BV1600	20	1.86	1.79	4,800
138-BV1600	35	1.81	1.77	5,200
138-BV1600	50	1.79	1.74	5,300
138-pitch	30	1.85	1.52	3,500
138-pitch	35	1.81	1.56	4,900
138-pitch	40	1.81	1.58	5,100
138-79L	20	1.79	1.62	1,600
138-79L	30	1.73	1.62	2,100
138-FA	40	1.65	1.55	600

(a) The first part designates the type of natural graphite described in Table 5-1. The second part designates the binder material as follows: BV1600: Bakelite phenolic resin; 79L: phenolic resin supplied by Old Ironsides Co; pitch: Barrett No. 2 medium hard pitch; FA: furfural alcohol.

(b) Average of 3 samples.

(c) Average of 2 samples.

(d) One sample tested.

TABLE 5-3

Density and Strength of Natural Graphite Pellets (2nd Series)

Graphite Composition [a]	Gms. binder per 100 gms of filler	Green Density g/cc[b]	Baked Density, g/cc[c]	Compressive Strength, psi[c]
6387-none	0	2.14	1.95	1,000[d]
6387-BV1600	5	2.01	1.96	1,800
6387-BV1600	10	2.00	1.95	4,800
6387-BV1600	15	1.99	1.88	3,300
6405-none	0	2.03[c]	2.06	1,900
6405-BV1600	5	2.12	2.06	3,100
6405-BV1600	10	2.09	2.01	2,700
6405-BV1600	15	2.04	2.02	3,500
6405-BV1600-10T	20	1.89	1.86	2,200
6405-BV1600-20T	35	1.79	1.70	2,700
6405-pitch-10T	40	1.82	1.51	2,500
6405-pitch-20T	35	1.84	1.56	2,200

(a) Designations are same as used in Table 5-2 except that -10T and 20T designate 10% and 20% thermax carbon black added to filler.
(b) Average of 3 samples.
(c) Average of 2 samples.
(d) One specimen tested.

As can be noted in Table 5-3, there has been some decrease in strength below the values shown in Table 5-2 for the higher binder contents. Maximum strengths in the lower binder content range appear to be at 10 parts binder with the 6387 graphite and 5 parts binder with the 6405 graphite. Additions of the thermax carbon black had little effect on the strength but did decrease the final density.

During the next quarter, it is planned to prepare some 1 1/2" spheres using the 6387 and 6405 graphities with 5 and 10 parts binder so that the impact strength, compressive strength, and abrasion resistance of these materials can be determined.

6.0 In-Pile Loop

The design and construction of an in-pile loop to study the behaviour of fission products escaping from a PBR fuel element was continued during this quarter under a subcontract to the Nuclear Science and Engineering Corp. The purposes of this loop are to study the equilibrium activity levels in a recycle helium stream; methods of lowering gas stream activity level; the amount, location, and nature of deposited fission products; and methods of decontaminating equipment surfaces. In addition to testing low-release PBR fuel element specimens, an uncoated uranium-graphite specimen will be tested to simulate problems of a "dirty" primary loop.

The in-pile portion of the loop will be inserted in experimental hole W-11 of the Brookhaven Graphite Reactor with the blowers, heat exchangers, sampling stations, etc. located on the adjacent floor space. Design characteristics of the loop are as follows:

Circulating Fluid	Helium
Operating Pressure	14 psia
Flow Rate	8 scfm
Max. Helium Temp.	1250°F
Min. Helium Temp.	250°F
Max. Specimen Temp.	1800°F
Max. Specimen Power	0.25 KW

Two major variables, the system pressure and the specimen power, have been selected with a view to minimizing the cost of the loop. The use of sub-atmospheric pressure eliminates the need for double containment while the modest power level in the specimen will provide measurable activity yet minimize the gas flow requirements and shielding costs.

Figure 6-1 is a schematic diagram of the in-pile loop. Gas leaves the in-pile section at 1250°F and enters the shell side of a coiled tube heat exchanger where it is cooled to 550°F. The exchanger is designed for easy replacement of the tube coil so that deposition on the tube surface as a function of temperature can be studied. An intermediate Dowtherm loop, which transports heat from this exchanger to a water-cooled sink, has been

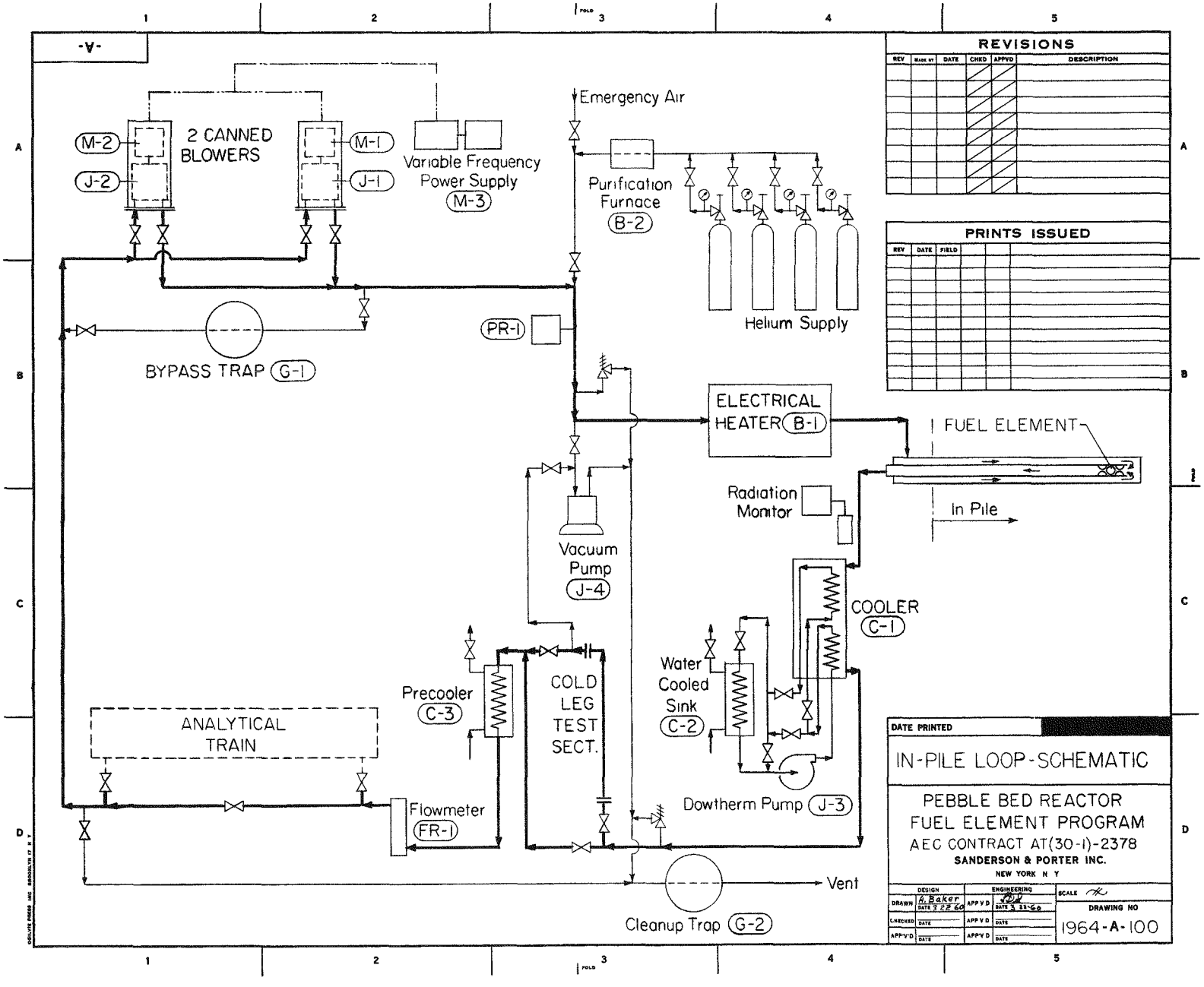

FIG. 6-1 UNCLASSIFIED

included to permit adequate control of the helium outlet temperature. The helium next passes through a removable 550°F test section and a precooler to lower the temperature to 250°F which enables the use of an economical low temperature blower. Before entering the blower, provision is made for in-line or bypass operation of an analytical train which will gather data on fission product release rate and activity levels in the gas stream.

Two Dexter-Conde positive displacement blowers are provided, although only one is required for normal operation. Each blower and its drive motor are mounted in a canned enclosure to provide a zero leakage system. Flow variation is achieved by powering the drive motors from a variable frequency motor generator set. A bypass charcoal trap is provided from the blower discharge back to the blower inlet so that the effect of continuous gas decontamination can be studied. After leaving the blower, the helium temperature is raised to 1200°F by an electrical resistance heater and then enters the in-pile section.

The in-pile section is designed for accommodation in a four inch square experimental hole. Co-axial flow is used in the in-pile region, while separated pipes are possible in most of the shield plug. A flange near the point where the inlet and outlet pipes become co-axial permits removal of the test specimen and high temperature plate-out coupons. A vacuum jacket insulates the co-axial section while fibrous insulation is used for the inlet and outlet pipes. The test specimen, a fueled 1-1/2 inch graphite sphere, is surrounded with portions of dummy spheres to simulate the flow pattern in a ball bed. Two thermocouples will be imbedded in the test specimen to permit accurate temperature measurement.

During this quarter, fabrication and subassembly of all components of the loop was completed and the components were shipped to BNL for final assembly. The out-of-pile portion of the loop was assembled in three sections at NSEC to facilitate shipment to BNL. Prior to insertion in the BNL reactor, the in-pile section will be connected to the out-of-pile section for pre-operational testing. A special graphite sphere containing a miniature 0.25 KW electrical heater will be used to simulate nuclear heating. This special sphere will also be used during the first cycle of operation so that loop compatibility with BNL operating requirements can be demonstrated in the absence of fission product activity. In-pile operation will commence during the next quarter.

The first fuel element to be irradiated in the loop will be an FA-22(E) specimen fueled with alumina coated UO_2 from batch 6H (see Table 2-1). This specimen will be otherwise similar to the FA-22 specimens being irradiated in Capsule SP-5 except for the provision of two thermocouple holes in the in-pile loop specimen. During fabrication of these specimens, small graphite plugs were molded into the sphere. After baking, thermocouple holes were drilled in these plugs so that none of the alumina coatings on the fuel particles would be damaged. Prior to insertion in the loop, a neutron activation screening test will be performed on the test specimen. Data on fission product leakage rates and volatile fission product concentration in the helium stream will be obtained. It is probable that the low release rates from the FA-22 specimen will make it difficult to obtain meaningful data on fission product deposition.

The second fuel element to be irradiated in the in-pile loop will be an FA-1(E) specimen fueled with uncoated UO_2 shot. Leakage factors of the order of 10^{-2} are expected from this type of specimen so it should be possible to obtain data on the efficiency of the bypass clean-up trap and fission product deposition in addition to measuring leakage rates and volatile fission product activity levels.

List of References

1. NYO 8753, Vol. I; Design and Feasibility Study of a Pebble Bed Reactor-Steam Power Plant; Sanderson & Porter; May 1, 1958.

2. NYO 2373; Progress Report on the Pebble Bed Reactor Program; Sanderson & Porter; June 1, 1958 to May 31, 1959.

3. NYO 2706; Phase I Progress Report on the Fuel Element Development Program for the Pebble Bed Reactor; Sanderson & Porter; May 1 to October 31, 1959.

4. S&P 1964-14; Quarterly Progress Report on the Fuel Element Development Program for the Pebble Bed Reactor; Sanderson & Porter; November 1, 1959 to January 31, 1960.

5. NYO 9058; Quarterly Progress Report on the Fuel Element Development Program for the Pebble Bed Reactor; Sanderson & Porter; February 1 to April 30, 1960.

6. Battelle Memorial Institute, Topical Report on Alumina Coated UO_2 Particles, to be published.

7. Battelle Memorial Institute, Topical Report on Pyrolytic Carbon Coated UC_2 Particles, to be published.